NANO LETTERS

Letter

pubs.acs.org/NanoLett

Reassessing Graphene Absorption and Emission Spectroscopy

Yuan Yang,[†] Grigory Kolesov,[‡] Lucas Kocia,[§] and Eric J. Heller*[,†,∥]

[†]Department of Chemistry and Chemical Biology, [‡]John Paulson School of Engineering and Applied Sciences, [∥]Department of Physics, Harvard University, Cambridge, Massachusetts 02138, United States

[§]Department of Physics, Tufts University, Medford, Massachusetts 02155, United States

Supporting Information

ABSTRACT: We present a new paradigm for understanding optical absorption and hot electron dynamics experiments in graphene. Our analysis pivots on assigning proper importance to phonon-assisted indirect processes and bleaching of direct processes. We show indirect processes figure in the excess absorption in the UV region. Experiments which were thought to indicate ultrafast relaxation of electrons and holes, reaching a thermal distribution from an extremely nonthermal one in under 5−10 fs, instead are explained by the nascent electron and hole distributions produced by indirect transitions. These need no relaxation or ad-hoc energy removal to agree with the observed emission spectra and fast pulsed absorption spectra. The fast emission following pulsed absorption is dominated by phonon-assisted processes, which vastly outnumber direct ones and are always available, connecting any electron with any hole any time. Calculations are given, including explicitly calculating the magnitude of indirect processes, supporting these views.

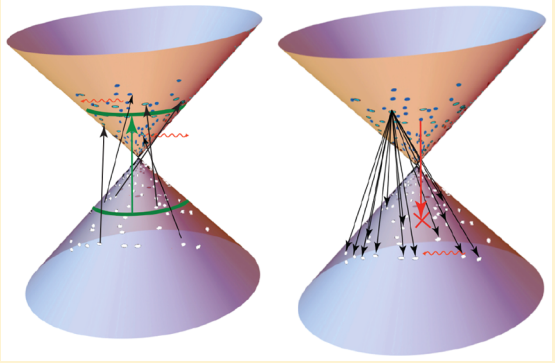

KEYWORDS: *Graphene, condensed matter spectroscopy, UV−vis spectroscopy, optical absorption, optical emission*

Graphene, with its sp^2-hybridized honeycomb two-dimensional carbon lattice consisting of conjugated hexagonal cells, shows extraordinary optical properties because of its dimensionality and unique electronic band structure.[1] As an atomically thin two-dimensional carbon material, graphene is used for transparent electrodes and optical display materials. It has also been applied in optoelectronics such as photodetectors, optical modulators, and so on.[2−12] A proper understanding of the carrier dynamics in graphene is key to its potential applications in high-speed photonics and optoelectronics. Many theoretical works concern the electron dynamics in graphene.[2,13,14]

In condensed matter theory, the electronic transition moments optically connecting valence and conduction band states are traditionally approximated as constant, independent of phonon displacement. In molecular spectroscopy this is called the Condon approximation. (To clarify this potentially confusing but established terminology, full Franck−Condon theory includes all phonon coordinate dependence of the electronic transition moment). We have found most of graphene spectroscopy falls into place naturally when full Franck−Condon theory is used; that is, it is essential not to use the Condon approximation. When phonons or in the case of molecules, vibrations are caused by the coordinate dependence of the transition moment, these are often called "non-Condon" effects. Recently, it was shown that indirect transitions induced by coordinate dependence of the transition moment (i.e., non-Condon effects) are responsible for the great intensity of some Raman overtones in graphene.[15] This is in line with traditional second-order Kramers−Heisenberg−Dirac Raman scattering theory, established in 1925−27.

In the present paper, non-Condon effects again play a central role for femtosecond pulse-probe absorption and femtosecond pulsed emission experiments, as well as traditional absorption spectroscopy. We show that no ultrafast relaxation is necessary or implied by a variety of experiments when these effects are included.

A significant body of published work supposes that ultrafast (5−10 fs) electron−electron relaxation follows ultrashort pulsed excitation. This seems to be an obvious inference: in a variety of experiments, one looks within femtoseconds after (one would think) creating an extremely nonequilibrium initial population, only to find the electrons behaving relaxed and even thermalized. For example, upon short pulsed excitation, graphene samples produce fast, readily observable light emission, appearing to be coming from a relaxed or even thermal distribution as soon as it can be seen, on the 7−20 fs time scale.[13,16,17] Ultrafast pump−probe absorption experiments similarly see probe spectra that appear to have no resemblance to the assumed narrow ranges of populated electrons and holes in the pump.[18]

Nonetheless, there have long been clouds on the horizon of the ultrafast landscape even without raising the issue of indirect,

Received: June 13, 2017
Revised: September 4, 2017
Published: September 5, 2017

DOI: 10.1021/acs.nanolett.7b02500
Nano Lett. 2017, 17, 6077−6082

non-Condon transitions. No experiment has ever caught a system in the act of the supposed ultrafast relaxation, nor any vestige of the putative ultrafast component. The relaxation times directly measured (rather than inferred by observing a relaxed looking distribution when first probed) in experiments have been in the 100−300 fs range, often attributed in the ultrafast literature to fast, but not ultrafast carrier−carrier or electron−phonon inelastic events, and a longer component in the 3−5 ps range, attributed to electron−phonon scattering. For example, saturable absorption (SA) experiments reveal unambiguously that the *fastest* time scale for electronic relaxation is 100−300 fs, not 5−20 fs, which agrees with earlier femtosecond pump−probe measurement on pyrolytic graphite.[19−21] The time scale for relaxation from an extremely nonequilibrium, saturated narrow band of energies to full thermalization could not be 10−20 fs or shorter, if saturation recovery takes 100−300 fs. Graphene has a reputation of being one of the easiest materials to saturate in absorption, except, importantly, for a significant nonsaturable component.[22] Its easy saturation and fast (not ultrafast) relaxation have earned graphene many trials and mentions as useful for solid state mode-locked lasers.

A serious storm cloud threatening the ultrafast narrative could be called the missing energy conundrum. In Lui et al.,[23] it is mentioned that the vertical energy per conduction electron at 1.5 eV (0.75 eV for the conduction band electrons) corresponds to an electron temperature of 9000 K. Once the assumption is made that the electrons and their emission are thermal just a few femtoseconds after the pulse, one is forced to arbitrarily remove 2/3 of the energy that has just been supplied to the electrons and use 3000 K electron temperature instead of 9000 to get a fit to the emission. This is a serious defect, since the fastest process and the only one effective on the few femtosecond time scale, namely, e−e scattering, cannot change the average energy per electron. The temperature becomes an adjustable, arbitrary fitting parameter, even though it should have been nonadjustable. Carrier multiplication might be suspected and was indirectly inferred and modeled as the only plausible explanation for what seemed to be 10 fs relaxation.[24] However, when carrier multiplication was was actually measured, it was not found to be present.[25] Also, if it exists somehow, it has stopped by the time probes are brought to bear, for further fast dumping of energy is not seen.

Seemingly in favor of the ultrafast relaxation idea are the beautiful experiments measuring electron coherence as seen by D-mode Raman scattering from a localized source, made visible after elastic backscattering from edges.[24] If the source of the conduction band electron was more than 8 nm round trip from the edge, or about 8 fs, the D-mode lost intensity due to lack of coherence with the hole. This was properly interpreted as a coherence length and dephasing issue, and not a measurement of the complete electronic inelastic electron relaxation time by any means.

Experimental results of disparate types fall into one unified picture if the emission and fast adsorption from a "thermal" electron and hole distribution is not due to ultrafast e-e relaxation. Rather, the distribution is nonthermal though widely distributed on the Dirac cones, and is nascent at $t = 0$ through a dominance of indirect transitions. These transitions, although present even for weak radiation, take over from the easily bleached direct transitions in a bright pulse. The myriads of possible indirect transitions we believe are responsible for the observed nonsaturable component.[22] To state it plainly, the electron−hole distribution is born pre-"relaxed" in bright pulsed absorption.

This new narrative is completed by consideration of how emission takes place. Non-Condon, phonon assisted indirect processes vastly outnumber and outweigh the possible elastic processes (Figure 1, right). Though individually weaker than the elastic channels, non-Condon indirect pathways are available from any electron to any hole at any moment. Direct emission on the other hand requires waiting for perfect momentum coincidence of randomly distributed electrons and holes. See Figure 1.

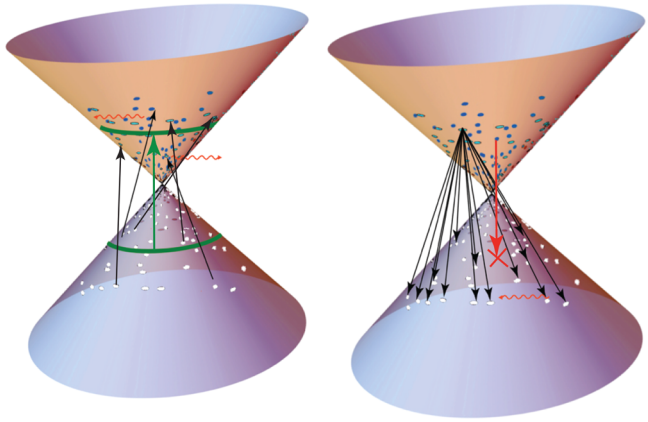

Figure 1. An illustration of mostly indirect optical absorption and emission processes in graphene: The left image shows two absorption mechanisms. The green arrow linking two green circles is a direct phonon-less absorption process from $-\hbar\omega_I/2$ in the valence band to $\hbar\omega_I/2$ in the conduction band, and the black arrows on the left linking holes and electrons are phonon assisted indirect absorption processes at the same vertical $\hbar\omega$ enabled by non-Condon effects. The right image shows the emission mechanism, leading to photons of energies from very low to up to $2\hbar\omega_I$. Any electron in the conduction band is ready for emission to any hole in the valence band by a phonon assisted transition, also enabled by non-Condon effects. It does not need to await perfect momentum alignment of randomly distributed electrons and holes. This is not overall the reverse of absorption, where a vacant conduction band state awaits every valence state and vertical energy is fixed. Conduction electrons are almost always Pauli blocked for direct emission (red arrow with X).

Following the implications of indirect absorption followed by indirect emission produces excellent agreement with fast emission and fast absorption experiments, without the need for arbitrary excited state energy removal, or any excited state relaxation at all on the femtosecond time scale (see below). Although this scenario is a long way from the prevailing consensus, it agrees with direct measurements of electron−electron relaxation rates from saturation experiments, mentioned above, and is free from the clouds and conundrums that the prevailing views are laboring under, also mentioned above. Indirect processes are hardly new in condensed matter spectroscopy, and we believe including them provides the missing link to understanding ultrafast graphene spectroscopy. Indirect processes are also part of the ordinary absorption excess in the UV (below).

Regarding ordinary CW light absorption, excess absorption over the "universal" value develops in the UV region.[17,26−28] We show here by explicit calculations that phonon-assisted transitions play an increasingly important role as the laser

DOI: 10.1021/acs.nanolett.7b02500
Nano Lett. 2017, 17, 6077−6082

frequency enters the UV region, contributing to the excess absorption in the UV.

In what follows, new results for graphene UV absorption are discussed first, where phonon-assisted processes are key. Then, we address the subject of fast spontaneous emission following bright pulsed excitation, showing that phonon-assisted processes explain the spectra without any relaxation. Finally we show that seemingly ultrarapid relaxation seen in pump−probe absorption experiments are instead the result of nascent electron and hole distributions via non-Condon phonon assisted processes.

In the Supporting Information, an expression is derived for the absorption cross section from an initial state $|i\rangle$ to a final state $|n\rangle$ as

$$\frac{\text{(energy/unit time) absorbed by the lattice } (i \to n)}{\text{energy flux of the radiation field}} \tag{1}$$

The absorption cross section from an initial state $|i\rangle$ to a final state $|n\rangle$ can be written in terms of the transition moment as

$$\sigma^{\hat{\epsilon}}_{i,n} = \frac{4\pi^2\hbar}{m_e^2\omega}\frac{e^2}{\hbar c}|\langle\chi_{\mathbf{m}_n}(\boldsymbol{\xi})|\mu^{\hat{\epsilon}}_{\mathbf{q}_c,\mathbf{q}_v}(\boldsymbol{\xi})|\chi_{\mathbf{m}_i}(\boldsymbol{\xi})\rangle|^2 \times \delta(E_n - E_i - \hbar\omega) \tag{2}$$

with the phonon coordinate dependent transition moment $\mu^{\hat{\epsilon}}_{\mathbf{q}_c,\mathbf{q}_v}(\boldsymbol{\xi}) = \langle\phi_{\mathbf{q}_v\mathbf{q}_c}(\boldsymbol{\xi};\mathbf{r})|\mathbf{D}^{\hat{\epsilon}}|\phi(\boldsymbol{\xi};\mathbf{r})\rangle_{\mathbf{r}}$, connecting the Born−Oppenheimer valence and conduction band electronic states, some with different phonon occupations, given by a matrix element of the dipole operator $\mathbf{D}^{\hat{\epsilon}}$ over the electronic states at the given nuclear positions. The wave function $|\chi_{\mathbf{m}_i}(\boldsymbol{\xi})\rangle$ is a particular nuclear wave function with phonons labeled by $\mathbf{m}_i$.

We use SIESTA to perform DFT calculations to get vertical phonon-less absorption and phonon-assisted absorption. To get meaningful physical quantities, we need wave functions having complete periods in our finite lattice, an 80 × 80 graphene supercell. Γ point wave functions in the supercell allow us to calculate both elastic and phonon assisted absorptions. It is important to point out that the non-Condon effects were not put in by hand or given an adjustable parameter, but rather *followed* from the electronic structure calculations and Franck−Condon matrix elements computed therefrom.

For direct, vertical absorption, we consider all electronic transitions from valence band to conduction band at the Γ point of the supercell Brillouin zone, and with electronic wave functions we can compute $\mu^{\hat{\epsilon}}_{\mathbf{q}_c\mathbf{q}_v}(\boldsymbol{\xi}_0)$. For indirect phonon-assisted absorption, we calculate $\frac{\partial\mu^{\hat{\epsilon}}_{\mathbf{q}_c\mathbf{q}_v}(\xi)}{\partial\xi_j}|_{\xi=\xi_0}$, that is, the change of transition moment under lattice distortion, by a finite difference method.

$$\frac{\partial\mu^{\hat{\epsilon}}_{\mathbf{q}_c,\mathbf{q}_v}(\boldsymbol{\xi})}{\partial\xi_j}|_{\xi=\xi_0} = \frac{\mu^{\hat{\epsilon}}_{\mathbf{q}_c,\mathbf{q}_v}(\boldsymbol{\xi}+\delta\xi) - \mu^{\hat{\epsilon}}_{\mathbf{q}_c,\mathbf{q}_v}(\boldsymbol{\xi}-\delta\xi)}{2|\boldsymbol{\delta\xi}|} \tag{3}$$

The numerator in eq 3 reads as the change of transition moment from an electronic state $\mathbf{q}_v$ to $\mathbf{q}_c$ when lattice is distorted from $-\boldsymbol{\delta\xi}$ configuration by $+2\boldsymbol{\delta\xi}$ to $\boldsymbol{\delta\xi}$. We use a diabatic approximation to the electronic states when the lattice is distorted by $+2\boldsymbol{\delta\xi}$ from $-\boldsymbol{\delta\xi}$, connecting the maximally overlapping adiabatic states, which have been recomputed after the change in nuclear displacements. (Recall that some lattice symmetry has been broken to make the displacements, so the old set of good quantum numbers do not otherwise make the connection obvious).

Graphene displays universal absorption in the near-IR region of 0.5−1.5 eV and a slow, at first quadratic rise above the universal absorption $\pi e^2/2h$, starting in the visible spectral region. There is a pronounced peak at E = 4.62 eV, dropping in the far UV region as in Figure 2. Our calculations as described

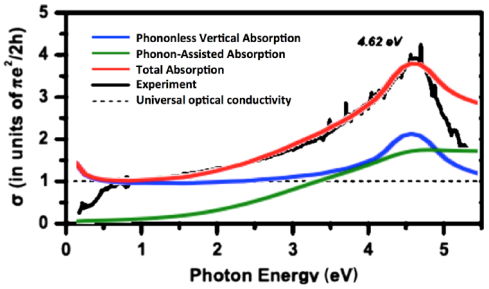

Figure 2. Calculated absorption curve vs experiment: The dark solid line is the experimental absorption curve adapted from the work of Mak etc.[30] The dashed line is the universal optical conductivity. The blue line is the calculated absorption contributed by direct phononless transitions; the green line is the calculated absorption from indirect phonon-assisted processes, and the red line is the total calculated absorption, summing the phononless transitions and phonon-assisted transitions. The coordinate dependence of the transition moment enables the indirect process. The failure of our calculated indirect processes to roll off sufficiently at high energy is not yet understood, except to say that the indirect processes remain well beyond the excitonic energy gap.

above and in the Supporting Information, with coordinate dependence of the transition moment included, show that, in the near-IR region, phononless direct absorption still dominates. Starting in the visible, phonon-assisted absorption starts to play an increasingly important role and is responsible for the quadratic rise in the near UV, with its influence increasing into the UV. The early rise starting in the visible is not justified by nonlinearities in the Dirac cones (see below), but nonlinearities do play a role at higher energies.

Assuming linear electronic dispersion, the density of electronic states for graphene is proportional to energy. For vertical phononless direct transitions, at a laser frequency $\hbar\omega$, an electron at $\hbar\omega/2$ below the Fermi level is excited to an empty state at $\hbar\omega/2$ above the Fermi level. There is a lone eligible conduction band electronic state for each occupied valence state, and the total number of vertical transitions is proportional to ω.

For phonon assisted indirect transitions, given a laser frequency $\hbar\omega$, the conduction band state can lie anywhere with $0 < e < \hbar\omega$, and the hole can lie anywhere with energy $\hbar\omega - e > 0$ below the Fermi level, as long as the vertical energy gap between any given e−h pair is $\hbar\omega$ minus the energy to create the associated phonon. The total number of phonon assisted processes is proportional to $\int_0^{\hbar\omega} e(\hbar\omega - e)de \propto \omega^3$. Even though the matrix element for each indirect process is small compared to that of a direct one, the cubic growth of the number of indirect processes with energy makes the phonon assisted contribution significant at higher laser frequency. The two processes are shown in Figure 1, left. In the absorption calculation, there is a $\frac{1}{\omega}$ factor, making the contribution of direct processes constant linear Dirac cone dispersion region. The contribution of the phonon-assisted processes is seen

DOI: 10.1021/acs.nanolett.7b02500
Nano Lett. 2017, 17, 6077−6082

rising at first as ω^2. The nonlinearity of the Dirac cone in the UV region enlarges the electronic density of states, contributing significantly to the UV excess absorption only above about 3 eV.

The calculations are based on a supercell with periodic boundary conditions, giving a uniform sampling in the Brillouin zone. There are sampling errors especially in the low energy region, where the number of states is insufficient to compensate the $\frac{1}{\omega}$ factor accurately, as seen in Figure 2. There is also a small error compared to the known universal optical absorption in the low energy region in Figure 2, but the fit is good enough to give us confidence in the numerics.

It is clear there are even higher level band structure calculations possible, including electron−electron interactions in the mean field,[29] and we hope our point about the key role of indirect processes will encourage them to be included at ever higher levels of electronic structure theory.

It is found in several experiments that "relaxed" photoluminescence takes place in the time scale of 10 fs.[16,18,23] These experiments were interpreted assuming both the absorption process and the emission process are purely phononless direct transitions.

The time scale for an electron−electron scattering process is on the order of several femtoseconds, and that for an electron−phonon scattering is on the order of picoseconds. Both time scales are too long to make the excited electrons, and holes reach full thermalization in the order of 10 fs. In previous work, a temperature much lower than the 9000 K the excited electrons should reach is used to fit the experimental emission spectrum; otherwise, there is a ludicrous fit to the data. This shedding of electronic energy is not explained[23] and makes the ∼3000 K temperature used simply a fitting parameter, and one not consistent with experimental conditions.

Furthermore, under the thermalization argument, the temperature should only depend on the incident laser fluence and not the laser frequency. Instead the experimental data shows the higher the frequency, the higher the temperature.[16]

In our theory the "thermal" (in quotes because it really is not thermal or relaxed) electron and hole distribution is produced nascently at $t = 0$ by a dominance of indirect transitions which, although present for weak radiation, take over from the easily bleached direct transitions in a bright pulse.[22] No relaxation is required of the nascent distribution to give the observed emission spectrum. To state it plainly, the electron−hole distribution is "born" pre- "relaxed". Furthermore, the emission thereafter is almost certainly via vastly predominant inelastic indirect channels, which are always available from any electron to any hole, and do not need to wait perfect momentum coincidence of randomly distributed electrons and holes.

We assume holes in the valence band and electrons in the conduction band are generated by phonon-assisted absorption, neglecting the matrix element variation for different transitions for simplicity. Then the probability of a conduction band state located at e above Fermi level occupied by an electron is proportional to the density of electronic states at $E_i - e$:

$$f(e) \propto (E_\mathrm{i} - e)H(E_\mathrm{i} - e)H(e) \tag{4}$$

where E_i is the incident light energy, and $H(x)$ is the Heaviside function. Similarly, the probability of a valence band state located at e below Fermi level occupied by a hole is proportional to the density of states at $E_\mathrm{i} - e$:

$$h(e) \propto (E_\mathrm{i} - e)H(E_\mathrm{i} - e)H(e) \tag{5}$$

Similarly, we ignore the matrix element variation for different transitions, simulating the emission by simple process counting. Then the phonon-assisted emission intensity at E_e when incident energy is E_i by processes counting is

$$\sigma(E_\mathrm{e}) \propto \int_0^{E_\mathrm{i}} \int_0^{E_\mathrm{i}} e_1 f(e_1) e_2 h(e_2) \delta(E_\mathrm{e} - (e_1 + e_2))\, \mathrm{d}e_1\, \mathrm{d}e_2 \tag{6}$$

where the total number of excited electrons at e above the Fermi level is $\propto ef(e)$ and the total number of holes at e below the Fermi level is $\propto eh(e)$. We plot eq 6 for different E_i''s, and a fit of the curve to experimental data is as Figure 3.

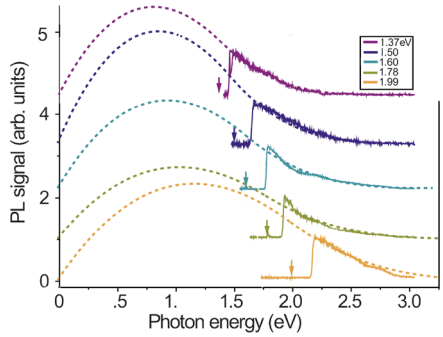

Figure 3. Emission spectrum with different incident laser frequencies: Solid lines are the experimental results of ultrafast photoluminescence from graphene under different excitation photon energies adapted from Liu.[16] Dashed lines are emission curves obtained from eq 6. No relaxation of the nascent electron−hole distribution or arbitrary energy removal is needed. Indirect absorption and emission, as in Figure 1, was used to calculate the emission spectrum, without adjustable parameters (save for the vertical scale, which was arbitrary in the experiment). Note two important features not explained by the ultrafast thermalization model but predicted by the indirect transition model: (1) The emission does not extend beyond energy $2\hbar\omega$ (because that is the maximum indirect process separation of electrons and holes). (2) There is movement of the high energy tail toward the UV as incident frequency is raised in the indirect mechanism, but the tail should be only fluence-dependent, not frequency-dependent, in the nearly instant thermalization model.

The expected laser fluence A dependence of the emission rate, assuming a purely indirectly produced e−h pump population and indirect emission, goes as A^2, exactly as seen in the experiments[13] at higher fluences. (Any electron able to emit to any hole with both populations proportional to A.) The experiments show an $\sim A^{2.5}$ dependence at lower fluences. This may be due to the onset of indirect process dominance as saturation becomes important. The indirect processes are too numerous to get saturated, but if the source of the electrons and holes is a direct process, saturation would cut off the quadratic A^2 rise at larger pump fluences. This fact alone weighs heavily against the "direct transitions followed by ultrafast relaxation" model.

In pump−probe experiments by Breusing et al., a starkly different probe absorption spectrum from that expected from the presumed pump e−h population leads to the understandable conclusion that ultrafast relaxation must have taken place in the femtoseconds between pump and probe. There is a totally different explanation involving indirect transitions that fits the data extremely well.

DOI: 10.1021/acs.nanolett.7b02500
Nano Lett. 2017, 17, 6077−6082

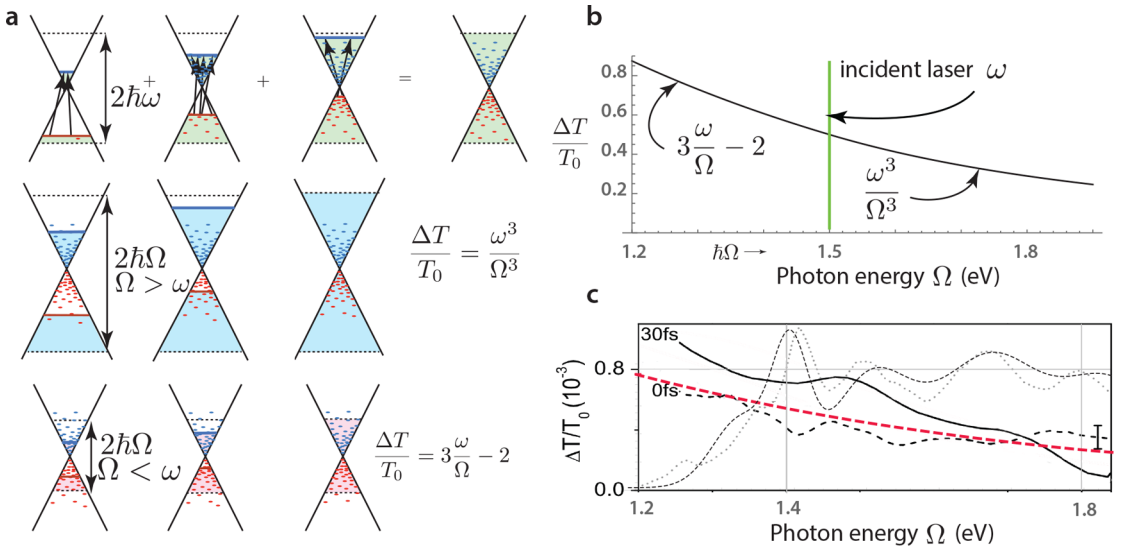

Figure 4. Explaining Breusing et al.[31] results without the need for relaxation. (a) (Top row) Production of the nascent e−h distribution by indirect processes in the pump stage. The dashed lines give the upper and lower bounds for the creation of electrons and holes at photon energy $\hbar\omega$, respectively. Transitions at $\hbar\omega$ (the total difference energy including created or destroyed phonons) connect the red and blue lines as they slide over the Dirac cones. The middle row shows the range of probe transitions at higher energy $\hbar\Omega > \hbar\omega$; all of the pump-produced electrons and holes separately induce missing processes in the probe pulse, inducing $\Delta T/T \propto \omega^3/\Omega^3$. In the bottom row, a lower energy probe photon $\hbar\Omega < \hbar\omega$ picks up only some of the electrons and holes produced by the pump as missing processes resulting in $\Delta T/T \propto 3\ \omega/\Omega - 2$. In b, the predicted probe absorption spectrum given a narrow band pump laser at $\hbar\omega$ is shown as a black line; there is no vestige of the pump profile even with no relaxation. After the pump c, a red dashed line shows the predicted probe spectrum assuming the first pulse had the spectral distribution of the thin dashed line; the experimental distribution is the gray dotted line. The experimental probe absorption spectrum is shown as dashed at 0 fs and solid at 30 fs.

The scenario is shown and explained further in Figure 4. Even a narrow bandwidth pump gives a probe absorption spectrum looking very much like the broad and dispersed experimental one (panel b in the figure), without any relaxation required.

There is no doubt that direct transitions are present, and we now address their impact. Because we have questioned the existence of ultrafast relaxation of the 10 fs variety, we assume the direct transitions are not much relaxed in the fastest experiments. For practical reasons, pump−spontaneous emission experiments must block emission at the incident laser wavelength, so they are not revealing about any direct emission from unrelaxed direct absorption. Pump−probe absorption is free of this problem, and indeed if direct probe absorption followed unrelaxed direct pump absorption then there should be an imprint of the pump profile on the probe. However, if 20% of the absorption is direct, and 20% of the probe is also direct, then only 4% of the probe absorption is direct−direct. The indirect signature of a direct component is a very diffuse transparency spectrum. Of greatest importance in this discussion is that the femtosecond pump and pump−probe experiments appear to be run deep in the saturated absorption regime (see, for example, ref 22).

An earlier pump−probe experiment on graphite, not privy to the relaxed-appearing spectral distribution, found a strongly biexponential decay, associating the faster decay with e−e relaxation, stating "the electronic system approaches an internal equilibrium with a characteristic time constant of 250 ± 50 fs".[19] The slower ps and longer decay was associated with e−ph scattering. In fact it needs stating that the more recent experiments also see these two time scales. It would appear therefore that three relaxation times scales are supposed: a sub 5−20 fs time scale, a 100−250 fs time scale, and a 1+ ps time scale. Here, we claim the sub 5−20 fs time scale does not exist and is an erroneous but very understandable inference from the deceptive indirect nascent e−h distribution.

There are two major goals of this work. The first is to provide alternative explanations and theoretical evidence suggesting that there is no ultrafast carrier relaxation in graphene implied by several important experiments, in spite of appearances. This is not a criticism of the experiments. Second, we seek to release the electronic transition moment from its traditional bondage (a principle that also drove recasting the theory of Raman scattering in graphene[15]), that is, to include non-Condon effects. If the electronic transition moment depends on phonon displacements (as it must), then phonons are produced (or destroyed) the instant a photon is absorbed, an inescapable fact within first-order light−matter perturbation theory within a Born−Oppenheimer framework.

The traditional frozen transition moment is badly misleading in graphene, but it is surely a reasonable approximation in many other situations. Still, these might profitably be re-examined with the electronic transition moment set free to look for non-Condon effects. A prime example are the indirect gapped transitions so important in many solids: it is known of course that a phonon is required to make these transitions allowed. Nearly every source we have checked leaves the matter there, as if a necessity or a momentum conservation law is an explanation of mechanism, which it is not. It seems likely to us that in many cases an explanation is the phonon coordinate dependence of the electronic transition moment, that is, non-Condon effects.

■ ASSOCIATED CONTENT

Supporting Information

The Supporting Information is available free of charge on the ACS Publications website at DOI: 10.1021/acs.nanolett.7b02500.

DOI: 10.1021/acs.nanolett.7b02500
Nano Lett. 2017, 17, 6077−6082

Derivation of direct and indirect absorption formul, which also includes more details on the methods of calculation and the phonon treatment. Calculated graphene phonon dispersion (Figure S1) and contribution to phonon assisted processes from different phonons (Figure S2) (PDF)

AUTHOR INFORMATION

Corresponding Author

*E-mail: heller@physics.harvard.edu. Phone: +1 617 449 8817.

ORCID

Yuan Yang: 0000-0001-9299-7941

Eric J. Heller: 0000-0002-5398-0861

Notes

The authors declare no competing financial interest.

ACKNOWLEDGMENTS

This work were supported by the STC Center for Integrated Quantum Materials, NSF grant no. DMR-1231319 and the Army Research Office Multidisciplinary University Research Initiative (MURI), award no. W911NF-14-0247. We used Odyssey cluster by the Research Computing Group at Harvard University and the Extreme Science and Engineering Discovery Environment (XSEDE), which was supported by NSF grant no. ACI-1053575. The authors thank professor Tony F. Heinz, professor Efthimios Kaxiras, Wei Chen, Shiang Fang, Wenbo Fu, and Ping Gao for helpful discussions.

REFERENCES

(1) Novoselov, K. S.; Geim, A. K.; Morozov, S. V.; Jiang, D.; Zhang, Y.; Dubonos, S. V.; Grigorieva, I. V.; Firsov, A. A. *Science (Washington, DC, U. S.)* **2004**, *306*, 666−669.

(2) Bonaccorso, F.; Sun, Z.; Hasan, T.; Ferrari, A. C. *Nat. Photonics* **2010**, *4*, 611−622.

(3) Kim, K. S.; Zhao, Y.; Jang, H.; Lee, S. Y.; Kim, J. M.; Kim, K. S.; Ahn, J.-H.; Kim, P.; Choi, J.-Y.; Hong, B. H. *Nature (London, U. K.)* **2009**, *457*, 706−710.

(4) Wang, X.; Zhi, L.; Müllen, K. *Nano Lett.* **2008**, *8*, 323−327.

(5) Bae, S.; et al. *Nat. Nanotechnol.* **2010**, *5*, 574−578.

(6) Vicarelli, L.; Vitiello, M.; Coquillat, D.; Lombardo, A.; Ferrari, A.; Knap, W.; Polini, M.; Pellegrini, V.; Tredicucci, A. *Nat. Mater.* **2012**, *11*, 865−871.

(7) Ju, L.; Geng, B.; Horng, J.; Girit, C.; Martin, M.; Hao, Z.; Bechtel, H. A.; Liang, X.; Zettl, A.; Shen, Y. R.; Wang, F. *Nat. Nanotechnol.* **2011**, *6*, 630−634.

(8) Liu, M.; Yin, X.; Ulin-Avila, E.; Geng, B.; Zentgraf, T.; Ju, L.; Wang, F.; Zhang, X. *Nature (London, U. K.)* **2011**, *474*, 64−67.

(9) Ren, L.; Zhang, Q.; Yao, J.; Sun, Z.; Kaneko, R.; Yan, Z.; Nanot, S.; Jin, Z.; Kawayama, I.; Tonouchi, M.; Tour, J. M.; Kono, J. *Nano Lett.* **2012**, *12*, 3711−3715.

(10) Lee, S. H.; Choi, M.; Kim, T.-T.; Lee, S.; Liu, M.; Yin, X.; Choi, H. K.; Lee, S. S.; Choi, C.-G.; Choi, S.-Y.; Zhang, X.; Min, B. *Nat. Mater.* **2012**, *11*, 936−941.

(11) Furchi, M.; Urich, A.; Pospischil, A.; Lilley, G.; Unterrainer, K.; Detz, H.; Klang, P.; Andrews, A. M.; Schrenk, W.; Strasser, G.; Mueller, T. *Nano Lett.* **2012**, *12*, 2773−2777.

(12) Zhang, M.; Zhang, X. *Sci. Rep.* **2015**, *5*, 8266.

(13) Mak, K. F.; Ju, L.; Wang, F.; Heinz, T. F. *Solid State Commun.* **2012**, *152*, 1341−1349.

(14) Heller, E. J.; Yang, Y.; Kocia, L. *ACS Cent. Sci.* **2015**, *1*, 40−49.

(15) Heller, E. J.; Yang, Y.; Kocia, L.; Chen, W.; Fang, S.; Borunda, M.; Kaxiras, E. *ACS Nano* **2016**, *10*, 2803−2818.

(16) Liu, W.-T.; Wu, S. W.; Schuck, P. J.; Salmeron, M.; Shen, Y. R.; Wang, F. *Phys. Rev. B: Condens. Matter Mater. Phys.* **2010**, *82*, 081408.

(17) Mak, K. F.; Sfeir, M. Y.; Wu, Y.; Lui, C. H.; Misewich, J. A.; Heinz, T. F. *Phys. Rev. Lett.* **2008**, *101*, 196405.

(18) Breusing, M.; Ropers, C.; Elsaesser, T. *Phys. Rev. Lett.* **2009**, *102*, 086809.

(19) Moos, G.; Gahl, C.; Fasel, R.; Wolf, M.; Hertel, T. *Phys. Rev. Lett.* **2001**, *87*, 267402.

(20) Kumar, S.; Anija, M.; Kamaraju, N.; Vasu, K.; Subrahmanyam, K.; Sood, A.; Rao, C. *Appl. Phys. Lett.* **2009**, *95*, 191911.

(21) Bao, Q.; Zhang, H.; Ni, Z.; Wang, Y.; Polavarapu, L.; Shen, Z.; Xu, Q.-H.; Tang, D.; Loh, K. P. *Nano Res.* **2011**, *4*, 297−307.

(22) Bao, Q.; Zhang, H.; Wang, Y.; Ni, Z.; Yan, Y.; Shen, Z. X.; Loh, K. P.; Tang, D. Y. *Adv. Funct. Mater.* **2009**, *19*, 3077−3083.

(23) Lui, C. H.; Mak, K. F.; Shan, J.; Heinz, T. F. *Phys. Rev. Lett.* **2010**, *105*, 127404.

(24) Brida, D.; Tomadin, A.; Manzoni, C.; Kim, Y. J.; Lombardo, A.; Milana, S.; Nair, R. R.; Novoselov, K.; Ferrari, A. C.; Cerullo, G.; Polini, M. *Nat. Commun.* **2013**, *4*, 127404.

(25) Gierz, I.; Petersen, J. C.; Mitrano, M.; Cacho, C.; Turcu, I. E.; Springate, E.; Stöhr, A.; Köhler, A.; Starke, U.; Cavalleri, A. *Nat. Mater.* **2013**, *12*, 1119−1124.

(26) Nair, R. R.; Blake, P.; Grigorenko, A. N.; Novoselov, K. S.; Booth, T. J.; Stauber, T.; Peres, N. M. R.; Geim, A. K. *Science (Washington, DC, U. S.)* **2008**, *320*, 1308−1308.

(27) Wang, F.; Zhang, Y.; Tian, C.; Girit, C.; Zettl, A.; Crommie, M.; Shen, Y. R. *Science (Washington, DC, U. S.)* **2008**, *320*, 206−209.

(28) Li, Z. Q.; Henriksen, E. A.; Jiang, Z.; Hao, Z.; Martin, M. C.; Kim, P.; Stormer, H. L.; Basov, D. N. *Nat. Phys.* **2008**, *4*, 532−535.

(29) Stauber, T.; Parida, P.; Trushin, M.; Ulybyshev, M. V.; Boyda, D. L.; Schliemann, J. *Phys. Rev. Lett.* **2017**, *118*, 266801.

(30) Mak, K. F.; Shan, J.; Heinz, T. F. *Phys. Rev. Lett.* **2011**, *106*, 046401.

(31) Breusing, M.; Kuehn, S.; Winzer, T.; Malić, E.; Milde, F.; Severin, N.; Rabe, J.; Ropers, C.; Knorr, A.; Elsaesser, T. *Phys. Rev. B: Condens. Matter Mater. Phys.* **2011**, *83*, 153410.

DOI: 10.1021/acs.nanolett.7b02500
Nano Lett. 2017, 17, 6077−6082